# FINAL PUBLISHABLE REPORT

| | |
|---|---|
| Grant Agreement number | 17IND01 |
| Project short name | MIMAS |
| Project full title | Procedures allowing medical implant manufacturers to demonstrate compliance with MRI safety regulations |

| | | |
|---|---|---|
| Project start date and duration: | | 01 June 2018, 40 months |
| Coordinator: Bernd Ittermann, PTB Tel: +49-30-3481-7303 E-mail: bernd.ittermann@ptb.de<br>Project website address: https://www.ptb.de/mimas/home | | |
| Internal Funded Partners:<br>1 PTB, Germany<br>2 INRIM, Italy<br>3 NPL, UK | External Funded Partners:<br>4 IOR, Italy<br>5 ZMT, Switzerland | Unfunded Partners:<br>- |
| RMG01: INRIM, Italy (Employing organisation); PTB, Germany (Guestworking organisation) | | |



**TABLE OF CONTENTS**


# 1 Overview

Medical implants represent a multi-billion market across Europe. A majority of the 50 million EU citizens carrying a medical implant will likely need a magnetic resonance imaging (MRI) scan during the lifetime of their device. However, the powerful electromagnetic fields of MRI systems in these cases represented a unique hazard for patient safety. Therefore, it was vital for both patient wellbeing and the success of a medical implant on the market that implant manufacturers could demonstrate safety compliance for their device in an MRI environment. This project improved the competitiveness of European implant manufacturers by providing innovative, metrologically sound and legally safe methods to demonstrate the compatibility of their products with MRI safety regulations.

New, high resolution anatomical models of implant carriers were developed, using virtual surgery techniques to position the device in the patient. A comparison to the less accurate, but simpler and cheaper state-of-the art techniques to create a computer of an implant patient is given. Researchers and implant manufacturers are, for the first time, to choose the proper approach to meet their specific requirements. A new *Medical Device Development Tools* was developed and regulatorily approved during the project. It is commercially available and provides implant manufacturers with a clear and legally safe pathway to obtain regulatory approval for their innovative devices. Beyond solutions for today, also completely new, and potentially disruptive approaches towards *personalised* implant safety assessments were investigated. On a proof-of-concept level it was demonstrated, how sensor-equipped implants interfaced to parallel-transmit capable MR scanners could not only combine patient safety with optimised image quality, but simultaneously make manufacturers more and clinical personnel less responsible for safety of an implant carrying patient. A complete assessment of the patient hazards due to gradient-induced heating of large implants in MRI was achieved and possible test procedures and simplified analyses were described. The ground is thus prepared for standardisation bodies to include this hitherto uncovered subject into their normative documents and for test laboratories to offer the relevant test procedures and equipment.

# 2 Need

With more than 30 million MRI scans per year across European countries, safety for patients with medical implants was a concern with some carriers having suffered fatal accidents due to the interference of their device with the electromagnetic fields (EMF) from the MRI scanner. MRI compatibility of an implant thus represented a key factor for the competitiveness of a manufacturer. This was exemplified in 2011 when Medtronic Inc. achieved the first ever MRI approval for a cardiac pacemaker and within a few years virtually all non-compatible devices disappeared from the market. However, the recently applied procedures to demonstrate MRI compatibility were either outdated (ASTM F2182) or incomplete (ISO/TS 10974). Additionally, large producers of high-end active implantable medical devices were facing technological challenges to demonstrate MRI compatibility, and SMEs manufacturing passive medical implants were overburdened by the necessity to demonstrate MRI safety for each new size and shape of a particular device, therefore limiting their innovation potential.

The established state of the art technique was and still is the numerical modelling of field distributions in human subjects. However, even though this technique has been used to include the presence of metallic implants, an experimental verification of the results was limited as mostly generic or simplified implants with non-detailed features were modelled. Parallel-transmit (pTx) radiofrequency systems can be used to steer, within certain limits, the electromagnetic field in MRI scanners as well as temperature distributions in and around the implant. The use of pTx for risk mitigation has an enormous potential to ensure safety for a wide range of different implants and boundary conditions. These systems can be combined with sensor-equipped implants to provide real-time feedback. However, this concept was still in an early stage of development and further work was needed to prove its usefulness.

The EMRP project ‘HLT06 MRI safety’ discovered that heating of metallic implants due to switched magnetic-field gradients was an underestimated hazard in MRI. As some normative documents ignored this effect completely, whilst others mentioned the possibility of such effects only in the context of protecting the device rather than the patient, this specific hazard was investigated in the project.

# 3 Objectives

To enable manufacturers of medical implants to demonstrate that patients carrying their products can safely undergo an MRI scan, the project aimed to achieve the following objectives:

1. To develop **anatomical models of human subjects with realistic medical implants** and millimetre resolution. The models to be sufficiently detailed for use with *in silico* medicine concepts, with resolution to be determined according to image analysis needs.
2. To develop validated computational tools for the **numerical simulation of electromagnetic fields (EMF) and temperature distributions** in a virtual human subject **during MRI exposure**. The computational tools should be able to process high-resolution anatomical models.
3. To develop validated methods and sensor-equipped reference implants for quantifying real-time implant-induced hazards during MRI exposure. This should include an assessment of parallel transmit (pTx) radiofrequency (RF) systems in MRI with real-time feedback and the **development of appropriate mitigation strategies**.
4. To investigate numerically and experimentally the hazards associated with **the interaction between bulk metallic implants and switched magnetic fields** in the kilohertz regime. In addition, to develop a reference set-up for testing metallic implant heating, using switched magnetic-field gradients of a few mT/m with a target gradient uncertainty below 5 %.
5. To develop and apply a **suitable statistical method to demonstrate MRI compliance** for small (< 10 cm) orthopaedic implants without extensive testing or numerical modelling, by determining an upper limit for the hazard associated with the new implant by comparison with a similar surrogate implant, which has already been fully assessed, thus enabling small manufacturers of a large variety of similar small metallic implants to dramatically reduce their costs for compliance demonstration.
6. To **interact closely with manufacturers of implants, MRI and test equipment and with standards developing organisations** (e.g., ISO/TS 10974, IEC TC/SC 62B and ASTM Subcommittee F04.15 on Material Test Methods) to align the project and facilitate the take up of the technology and measurement infrastructure developed in the project.

# 4 Results

## *4.1 Development of anatomical models*

*Relevance of the work carried out to meet the first objective*

Safety testing of metallic implants for MRI is largely based on unreliable phantom measurements. The project aimed to improve this unsatisfactory state of the art by applying more meaningful numerical modelling of realistic virtual models.

Objective 1 of the project was on the development of anatomical models of human subjects with realistic medical implants and millimetre resolution. In total, at least twelve device models had to be considered, with representative models for each type of medical implant (orthopaedic, long one-dimensional, small implants).

Therefore, new virtual models of human subjects carrying selected metallic implants have been developed. For the first time precision planning tools from virtual surgery were applied to position the implants with sub-mm accuracy. These hi-resolution realistic virtual models were widely used for all the numerical simulations throughout the project.

*Work undertaken by the partners*

All the activities necessary to reach the Objective 1 have been reported in detail in the Deliverable D1, led by IOR in collaboration with NPL and ZMT (Technical report: “Report on the development of anatomically correct digital models of the body carrying realistic medical implants”). Objective 1 required to develop anatomically correct digital models of human subjects carrying one of the following three categories of medical implants:

- massive orthopaedic implants like hip, knee and shoulder arthroplasties: activity led by IOR, in collaboration with INRIM and ZMT;
- long one-dimensional implants, like leads and electrodes of pacemakers and stimulation devices: activity led by ZMT;

- small stand-alone implants with the largest extension of 10 cm, like copper intrauterine devices (IUD), stents, aneurism clips, screws, plates and other fixation elements: activity led by NPL, in collaboration with INRIM, IOR and ZMT.

Implant selection was based on a prevalence analysis of different implant categories in the population, and by considering the heating risk for patients when submitted to MRI. The following implants were selected for the three categories:

- massive orthopaedic implants: hip, knee and shoulder arthroplasty;
- long one-dimensional implants: pacemaker (PM), deep brain stimulator (DBS), and spinal cord stimulator (SCS);
- small stand-alone implants with the largest extension of 10 cm: surgical staples, plates, and orthopaedic screws.

Consortium partner ZMT made the Virtual Population (ViP) models available to the project, a family of highly detailed whole-body virtual human models for dosimetric and biomedical applications (*https://itis.swiss/virtual-population/virtual-population/overview/*) which they had developed earlier in collaboration with the IT'IS Foundation. The ViP family includes different detailed, high-resolution anatomical models, created from MRI data of volunteers. The models differ for age, sex, and size of the body.

The most appropriate ViP models were chosen by the best match with the population with the different categories of implants:

- massive orthopaedic implants: GLENN, YOON-SUN
- long one-dimensional implants: GLENN, FATS
- small stand-alone implants with the largest extension of 10 cm: GLENN, YOON- SUN, DUKE.

The high-resolution anatomical models were used, from ViP Version 3, with an isotropic spatial resolution of 0.5 mm.

A great variety of surgical procedures were simulated, with the implant of the CAD models of medical devices on to the selected human models of the ViP family.

- For the massive orthopaedic implants, a total number of twelve surgical procedures were simulated, by combination of three types of implants (hip, knee and shoulder arthroplasty), applied on the GLENN and YOON-SUN body models, on both right and left anatomical sides.
- For long, one-dimensional implants, six anatomical models were provided by combining the two models FATS and GLENN with three implanted devices: pacemaker (PM), deep brain stimulator (DBS), and spinal cord stimulator (SCS).
- For small stand-alone implants, a proximal humeral plate was placed on the GLENN and YOON-SUN body models. Staples were placed on the inner side of the left tibia of GLENN and YOON-SUN. A variety of surgical screws were inserted into the DUKE model in clinically relevant locations.

These high-resolution sub-millimetre anatomical models carrying medical implants were therefore available for the numerical simulations of the project.

Activities planned to address Objective 1 were jointly pursued by an interdisciplinary team, capable to approach a mix of interlaced problems coming from numerical simulations, modelling of human body and surgical procedures. In details the following partners were involved:

INRIM's experience is mainly focused on modelling aspects related to electromagnetic dosimetry. INRIM strongly interacted with IOR and ZMT in the definition of the most interesting scenarios for massive orthopaedic implants and gradient coil heating.

IOR is a public orthopaedic-only hospital. It has a long tradition in prosthetic devices for the articular joints (hip, knee, shoulder, ankle) and in musculoskeletal radiology. IOR provided to the team the clinical knowledge to investigate the prevalence of patient with orthopaedic implants and submitted to MRI scan, and for virtual surgery in orthopaedics. IOR coordinated the activities for Objective 1.

NPL has established test facilities to assess the RF heating of implants. NPL led the activities regarding small stand-alone implants, in collaboration with INRIM, IOR and ZMT.

ZMT is currently the leading provider of test and evaluation systems for demonstrating MR safety of passive and active implants. The Virtual Population (ViP) models, a family of highly detailed whole-body virtual human models developed at ZMT and IT'IS foundation, have been provided for the aims of the project. ZMT led the activities regarding long one-dimensional implants.

The excellent collaboration between the partners guaranteed the achievement of the expected results related to Objective 1.

*Summary of key outputs and conclusion*

Medical implants were selected, and the surgical procedures were simulated on the best candidates from the Virtual Population (ViP) models, a family of highly detailed whole-body virtual human models. High-resolution anatomical models were used from ViP Version 3, with spatial resolution of 0.5 mm x 0.5 mm x 0.5 mm.

For the massive orthopaedic implants, a total number of twelve surgical procedures were simulated by the placement of hip, knee, and shoulder prostheses, on either anatomical side of two body models.

For long one-dimensional implants, six anatomical models were provided by the placement of pacemaker, deep brain stimulator, and spinal cord stimulator on two body models.

For small stand-alone implants, surgical staples and plate were placed on two body models. A variety of surgical screws were also inserted in a third selected body model in clinically relevant locations.

High-resolution CAD files of the anatomical models with realistic implants were made available for the aims of the project. The targets related to Objective 1 of the project were therefore achieved, providing a significant progress beyond the state of the art.

## *4.2 Electromagnetic simulations*

*Relevance of the work carried out to meet the second objective*

Objective 2 of the project was to develop validated computational tools for the numerical simulation of electromagnetic fields (EMF) and temperature distributions in a virtual human subject during MRI exposure. To meet this objective, the work had to be broken down into distinctive steps: i) the computation of a library of the incident fields generated by the MRI scanner in the subjects' body when an implant is not yet present.; ii) the automatic extraction of fields along the implant's trajectory, iii) modelling of the implant's electromagnetic response; and iv) simulations of the induced temperature rise.

*Work undertaken by the partners*

*Incident Fields*

For a comprehensive assessment of implant safety under MRI exposure, potential clinical scenarios need to be recognised and considered during the assessment. A literature survey has been conducted to compare the characteristics of the implanted patient population with those of the Virtual Population (ViP) models developed by IT'IS Foundation. Experimental surveys of commercial MRI scanner RF coils were conducted, and the findings with respect to the physical parameters of the RF coils are summarised in Table 4.2.1.

| Manufacturer | Model | Bore size (cm) | Coil length (cm) | Shield length (cm) | No. of rungs |
|---|---|---|---|---|---|
| Siemens | Prisma 3.0T | 60 | n/a | <200 | n/a |
| Siemens | Skyra 3.0T | 70 | 50 | <100 | n/a |
| Siemens | Spectra 3.0T | 60 | n/a | <175 | n/a |
| Siemens | Verio 3.0T | 70 | 45 | <120 | n/a |
| Phillip | Achieva 3.0T | 60 | 40 | <160 | 16 |
| Phillip | Ingenia 3.0T | 70 | n/a | n/a | n/a |
| Phillip | Ingenia CX 3.0T | 60 | n/a | n/a | n/a |

| | | | | | |
|---|---|---|---|---|---|
| GE | Twinspeed 3.0T | 60 | 70 | <105 | 24 |
| Siemens | Avanto 1.5T | 60 | 55 | <60 | 16 |
| Siemens | Espree 1.5T | 70 | 45-55 | <120 | 16 |
| Phillip | Achieva 1.5T | 60 | 50-60 | <60 | 16 |
| GE | Twinspeed 1.5T | 60 | 60 | <70 | 16 |

*Table 4.2.1: Physical dimensions of the cylindrical RF (birdcage) coils.*

In Figure 4.2.1, the age and BMI for the available anatomical models, and the estimated range for different implants are illustrated. For a comprehensive assessment, anatomical models with different gender, BMI range of 13-40 (kg/m2), age range of 4-90 years old should be considered. Based on the experimental survey, RF coils with coil length from 50 cm to 80 cm, diameter of 60 cm to 80 cm should be considered.

To include these potential clinical scenarios, numerical simulations of exposure scenarios with:

1. 64 MHz and 128 MHz,
2. 10 RF coils with coil length of 40 to 70, diameter of 65 to 80,
3. anatomical models of different sexes,
4. anatomical models with BMI range of 13.8 – 36 (kg/m$^2$),
5. anatomical models with age range of 6 – 84 years old,
6. imaging positions from head to feet with resolutions of 5 cm and 2.5 cm

were performed. The resulting field datasets, the MRIxViP1.5T and MRIxViP3.0T libraries depict the RF-induced electric and magnetic fields within the anatomical phantoms of the Virtual Population during exposure to RF of 1.5T and 3.0T MRI. The libraries, when used in combination with appropriate data analysis tools, can provide relevant parameters of merit from which patient safety is derived.

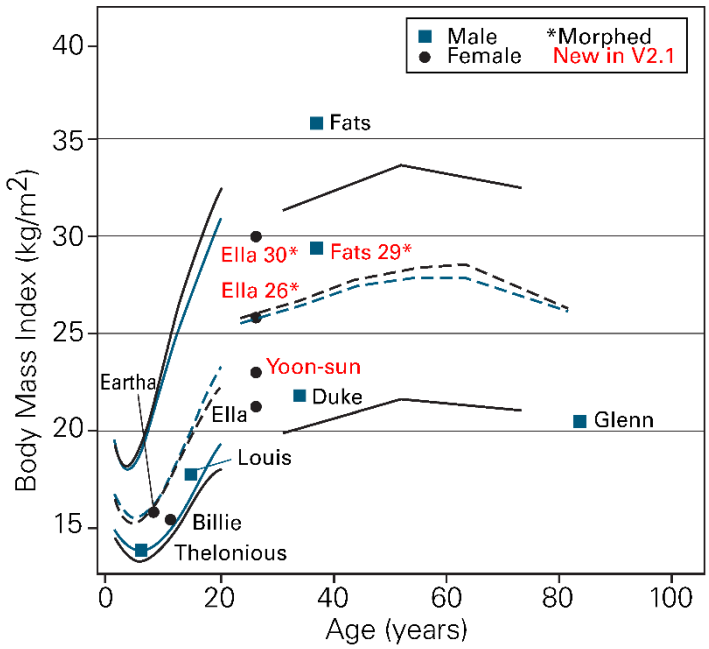


*Figure 4.2.1: Illustration of age and BMI for the available anatomical models and the estimated rage for different implants. The lines represent the statistical distribution of the population (mean: dashed line; 95th percentile: solid lines). Sources: 2 – 20 years from National Center for Health Statistics (doi:10.1001/jama.2014.732); 25 – 80 years approximated from Ogden et al. (PMID: 15544194).*

*Field Extraction*

ZMT developed IMAnalytics, an extraction and evaluation tool which generates a mathematically correct result, namely the E-fields in human computational models in a region of interest or along a clinical routing, when used together with a database of patient exposures (such as the MRIxViP database). These E-fields, averaged over a volume (typically 10g of tissue) or a clinical routing, can be used as an input for safety evaluations, and/or to determine the power deposition at an implant hotspot or induced voltage in a lead channel terminal, with a valid transfer function model of implant response.

The in vivo RF exposure data libraries MRIxViP 1.5 and MRIxViP 3.0T and the standardised evaluation tool IMAnalytics have been accepted by U.S. Food and Drug Administration (FDA) as a Medical Device Development Tool (MDDT). The MDDT label of the tools certified that evaluations of the health risk posed by medical implants to patients undergoing magnetic resonance imaging (MRI) diagnostics are traceable, easy-to-conduct, and standardised at the most comprehensive level. T combination of IMAnalytics and MRIxViP data libraries enables the medical device industry to accelerate the approval process with high quality of risk evaluations.

To verify the tool's effectiveness and workflow, numbers of generic and realistic implants, ranging from generic plates and screws, to samples of real passive implants, to a generic active implant developed for test method validation (the SAIMD-U, Figure 4.2.2) were selected for study. For each implant category, a region of interest (ROI) has been defined inside each of the selected anatomical models (Glenn and Yoon-sun) as shown in Figure 4.2.3; while clinical routings corresponding to implants are shown in Figure 4.2.4.

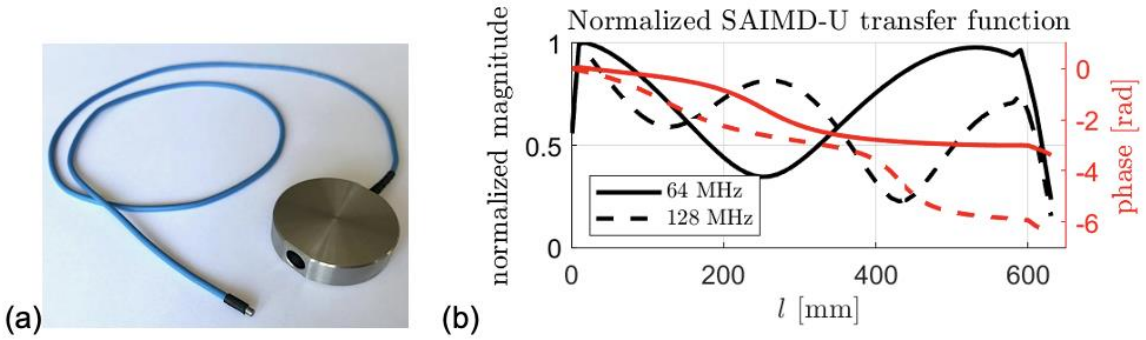


*Figure 4.2.2: Generic implant used for comparison: (a) photograph of SAIMD-U (ZMT) and (b) transfer function at 64 MHz (solid lines) and 128 MHz (dashed lines). The normalised magnitude is shown in black and the phase in red.*

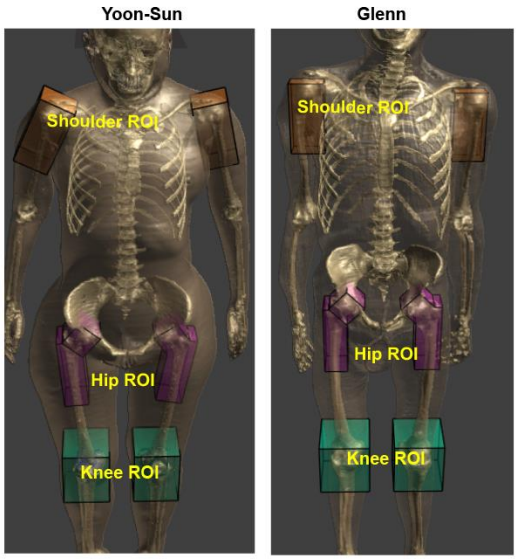


*Figure 4.2.3: Region of Interest (ROI) in Yoon-Sun and Glenn.*

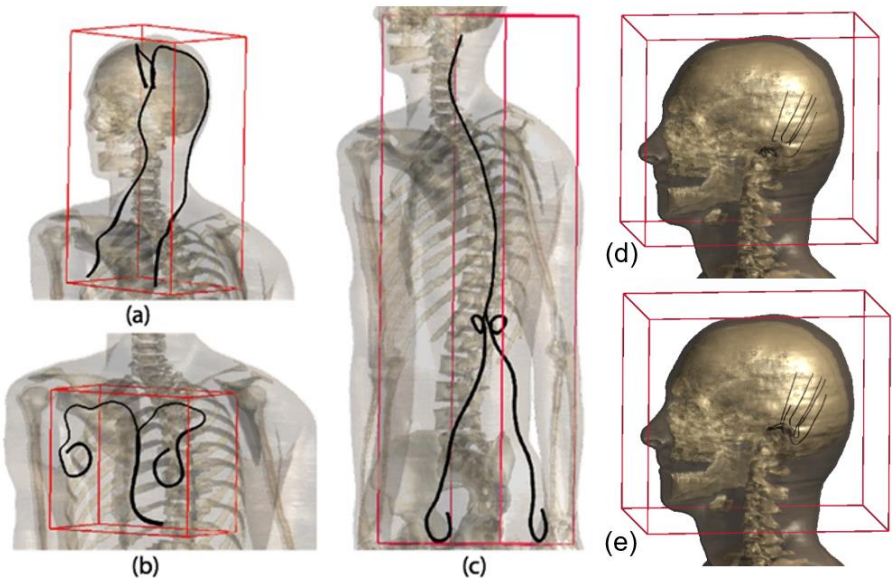


*Figure 4.2.4: Sample trajectories in ViP model Duke for (a) DBS, (b) pacemaker, (c) SCS, (d) intracochlear, (e) extracochlear AIMD.*

The maximum 10g-averaged electrical field (E10g) within each ROI has been computed and extracted. The averaging over any 10g of tissue as described in IEEE C95.3 is implemented by the tool. More than 300 clinical scenarios are selected for each anatomical model under each frequency (64 MHz and 128 MHz), including 10 RF birdcage coils, 17 imaging positions from head to feet with a step of 10 cm, and 2 typical clinical scenarios (left-hand circular and right-hand circular).

*Implant Modelling and Response*

To numerically apply the estimated in vivo incident fields to electrically short implants, a generic in vitro model has been proposed, which allows a simplified but not overly conservative assessment of RF safety of electrically short implants. The approaches can be decomposed into 2 steps: a) assessment of the maximum in vivo incident E-field in the ROI according to Tier 2 of ISO 10974; and b) place the implant in a simplified tissue model conservatively representing the implant's tissue environment, and excite the implant with a uniform incident E-field with the maximum average strength derived from a).

To demonstrate this, coupled EM and thermal simulations of selected short implants were performed using the simplified simulation model, and the results were normalised to the maximum in vivo incident level. The following categories of small passive implants have been defined for study by the team:

1. Titanium Rods with length of 20- 100 mm, diameter of 1 – 10 mm,
2. Screws with length of 10 – 100 mm,
3. Plates with size of 50 mm x 100 mm, and 100 mm x 100 mm, thickness 1 mm,
4. Stents with 20 – 100 mm length.

The RF-induced power deposition and temperature rise were found to vary greatly as a function of implant geometry. The worst-case clinical incident field condition (highest peak spatial SAR) was anatomical phantom Yoon-Sun exposed with RF coil B65_L70, at imaging position 15 (foot scan), with left-hand circular polarisation at 64 MHz. The Tier 4 simulations of the worse-case clinical scenario were performed with the 100 mm implant screw implanted inside the human model. In vitro SAR and temperature measurements were also performed and compared between laboratories and to numerical results in homogenous medium.

For active implants (AIMD), the Tier 3 approach was used, and the approach description integrated into an informative annex of the current working draft of ISO 10974. The Tier 3 AIMD electromagnetic mode uses piecewise excitation of the AIMD immersed in tissue simulating medium by an exciting antenna at the target frequency, and measurement of the response as the exciting antenna is swept along the length of the AIMD. Experimentally, coupling between the exciting antenna, the AIMD, and the sensor measuring the AIMD response should be minimised through appropriate design and feeding of the exciting antenna, appropriately isolated sensors, and appropriate phantom size and boundary conditions. The incident field to which the implant is exposed piecewise should be kept consistent as the exciting antenna is moved along the length of the device, so that the relative magnitude and phase of the AIMD response can be accurately measured for each segment. For E-field measurements, the incident E-field to the sensor from the exciting antenna must be subtracted. An alternative approach utilises the principle of reciprocity together with the Huygens Principle to invert the system, placing the current source at the lead tip and measuring the current distribution along the AIMD length. Experimentally, coupling between the current injection system and the AIMD, and the sensor measuring the AIMD response must similarly be minimised. The scaling factor of the transfer function response may be directly extracted from the measurement or simulation, or derived separately via a radiated exposure to a known incident field. These transfer functions were numerically derived and experimentally validated for the SAIMD-U wire derived for this purpose (Figure 4.2.2).

The impact of anatomical variation on medical implant risk assessment of devices was demonstrated for generic transfer functions and lead trajectories representing pacemaker, DBS, SCS, and cochlear implant routings. Depending on the implant type and location, and the imaging landmark, the maximum deposited power could occur in any of the 12 anatomical models, even when considering only one generic transfer function (the SAIMD-U). This variability supports the fact of a large anatomical dependence of the induced fields, which are difficult to predict, and therefore the safety of patients with implants is best warrantied when a large number of independent anatomical models are evaluated when defining the safety envelope of MR compatibility of AIMD.

The confidence interval of ISO 10974 Tier 3 evaluations of deposited power around specific absorption rate (SAR) hotspots in tissue, or induced voltage in a channel, is assessed for elongated medical implants with the ISO 10974 Tier 3 method. The confidence interval estimation follows the methodology of the GUM and comprises uncertainty terms from measurement as well as supporting simulations.

*Temperature Rise and Thermal Dose*

Transient local peak temperatures of radiofrequency induced local thermal hotspots within a 1.5T body coil were numerically and experimentally assessed as a function of exposure level and local thermoregulation in four anatomical human models in different Z-positions. To quantise the effective thermal stress of the tissues, the thermal dose model cumulative equivalent minutes at 43 C (CEM43) was employed, allowing the prediction of thermal tissue damage risk and the identification of potentially hazardous MR scan-scenarios. The numerical results were validated by $B_1^+$ and skin temperature measurements.

As part of the MIMAS project, ZMT and partner IT'IS Foundation hosted the Thermal Dose Workshop 2019 at Z43 on April 2–3, 2019, gathering experts from around the globe to discuss critical safety issues in magnetic resonance imaging (MRI). Participants from industry – including representatives of MRI manufacturers –

medicine, and academia packed the third-floor meeting room for two days of presentations on a wide range of pertinent topics and focused discussion to guide decisions on the best safety limits for MRI and how to implement them. The first day of the workshop was dedicated to finding the thermal limits, with presentations on mathematical models of heat stress, the molecular biology of the heat-shock response, local and systemic effects of thermal stress, epidemiology, and theoretical and practical aspects of the cumulative equivalent time at 43°C (CEM43) concept. During the second day, approaches to reasonable implementation guidelines to ensure compliance with the basic restrictions in the standard, including discussions of uncertainty, were covered. The overall consolidation of reports and conclusions was that nothing important was missed in the relationship between temperature rise, thermal dose (CEM43) and tissue damage and their applicability to relevant standards, should this be implemented.

*Summary of key outputs and conclusion*

ZMT, together with partner IT'IS Foundation has developed, validated, and received FDA qualification for the tools used to predict the EMF distributions in 12 anatomical models of the Virtual Population for a set of 10 RF birdcages at 1.5T and at 3T covering the range of commercial high-pass closed-bore scanners. In brief, the induced E-fields and $B_{1,\mathrm{rms}}^{+}$ fields from exposure to RF body coils from head to feet imaging landmarks over the full polarisation space were estimated via the verified EM-FDTD solver of Sim4Life. The target of estimating the local SAR, the maximum averaged E-field over any 1 $cm^3$ cube of tissue (E1cm3), and the tangential E-field (Etan) for relevant implant trajectories is achieved, and the toolset qualified by the US FDA on the basis of the verification and validation evidence provided as part of the Medical Device Development Tool program. Estimates of the deposited power from an ISO 10974 Tier 3 or Tier 2 evaluation can be translated to local temperature rise and thermal dose with the IT'IS Tissue Property Database and the verified Thermal solver of Sim4Life, which was validated experimentally by measurements of generic implants in collaboration with NPL. This report compiles and summarises the verification and validation evidence accumulated for each piece of this toolchain.

Existing assessment methods for the MRI RF safety of metallic implants have been adjusted, enhanced, and tailored for the specific needs of this project. The induced electric field maps for newly developed anatomical human models have been computed, which will allow to perform adequate evaluations for the investigated implant categories. The joint effort in identifying and categorising relevant medical implants allows to perform all relevant safety assessments at and beyond the state of the art. Methods for simplified and accurate estimations have been developed, including an iso-electric exposure scenario within tissues of different relative permittivity (e.g., water-like, fatty, bone) and on their interface (e.g., orthopaedic implants on the bone-muscle interface).

### *4.3 Mitigation of implant induced hazards using real-time sensor measurements and parallel transmit radiofrequency systems*

*Relevance of the work carried out to meet the third objective*

The concept of E-field steering using parallel transmission (pTx) to mitigate implant-related risks in MRI was evaluated at the research level, with the result that a very high potential was identified, in particular for smart implants. But their translation to the clinical routine can be attempted only with a much deeper investigation which this project aimed to perform. Thus, there was an urgent need to develop a portfolio of simulation-based evaluation methods for radiofrequency (RF) induced thermal effects. It was clear from the very beginning that only a sensor-based method would be able to provide the necessary measurement data to actively mitigate RF heating at the implant tip. In order to ensure robust and reliable results the development of validation methods using sensor-equipped reference implants is required. For practical implementation, it is crucial that the pursued approach is real-time capable, patient and exam specific and solely based on the embedded sensor signals.

*Work undertaken by the partners*

In this project:

- methods to derive simplified numerical models of wire-type implants have been developed,
- a simulation framework was established allowing to perform the risk assessment for implants in pTx MRI machines,
- a dedicated pTx testbed has been designed, constructed, and commissioned,

- a clinically relevant safety concept based on smart sensor equipped implants was developed,
- an experimental setup based only on RMS sensors embedded in an implant was implemented that allowed this safety strategy for pTx-based MR systems to be put into practice,
- detailed measurements have been carried out to demonstrate the performance of sensor-based pTx-mitigation in mock implants.

The main approach pursued in the context of Objective 3 is the use of wire-type implants with embedded sensors which are capable to measure safety relevant parameters like temperature rise or point SAR. These sensors would allow a real-time feedback of such sensor measurements to actively control the heating related hazards by adjusting the pTx settings of the MRI scanner.

The work in the project was carried out by PTB together with contributions from ZMT. In addition, work was performed as part of an RMG by partner INRIM.

*Simplified numerical models of wire-type implants*

To implement an efficient simulation framework a simplified approach for the simulation of more complex wire type implants was developed using a full-scale simulation of a reference implant. To this end, the well-established SAIMD-U reference implant from ZMT was utilised. A comparison of detailed simulations of a 300 mm long SAIMD-U lead with electrode length of 10 mm and a simplified model was performed by ZMT. The simplified model uses the same insulation, but with much coarser grid resolution of 2mm x 2mm x 5mm instead of 0.1mm x 0.1mm x 1mm.

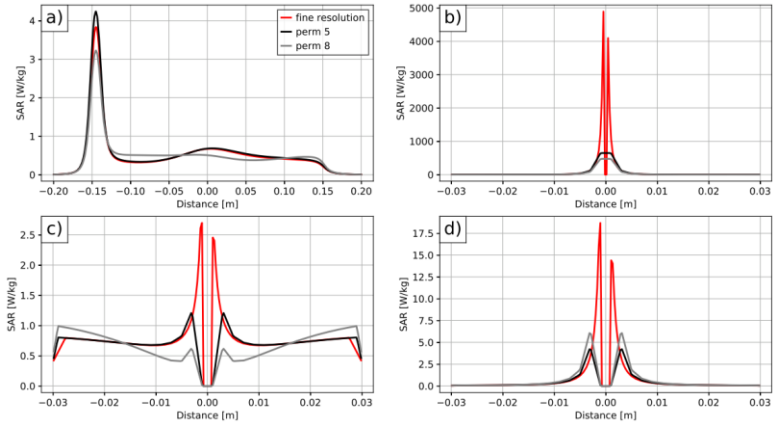


*Figure 4.3.1 Comparison of selected SAR profiles of SAIMD-U reference implant*

As can be seen from the SAR profiles in Figure. 4.3.1, a good matching of the simplified wire to the full-scale approach can be achieved by adjusting the dielectric permittivity of the insulation to a value of 8. Due to the underlying principle, there are stronger deviations in the immediate vicinity of the implant, but this is not relevant for the further simulation calculations.

*Simulation framework for the risk assessment of implants in pTx MRI machines*

A generic pTx birdcage body coil was modelled in Sim4Life 5.0 using the dimensions of a 3 T 70 cm bore system. A human voxel model from the 'Virtual Family' (e.g., 'Duke', doi: 10.13099/VIP11001-03-1-1) was inserted with the heart typically centred along the head-foot direction. For each configuration (e.g., patient position, implant length, etc.) two simulations were carried out: without implant and with implant. For the simulation with implant a wire was added with its tip located at the spinal cord. This wire was simulated using the simplified model as described above. For each simulation 48 single port excitation FDTD runs were performed at a frequency of 128 MHz resulting in 48 3D data sets of complex E and H-fields with 2mm spatial resolution (>200GB of data). The 8-channel coil field configurations were obtained by proper setting the voltages for each of the 8 channels at each of the 48 ports followed by superposition of the electromagnetic fields (see Figure 4.3.2).

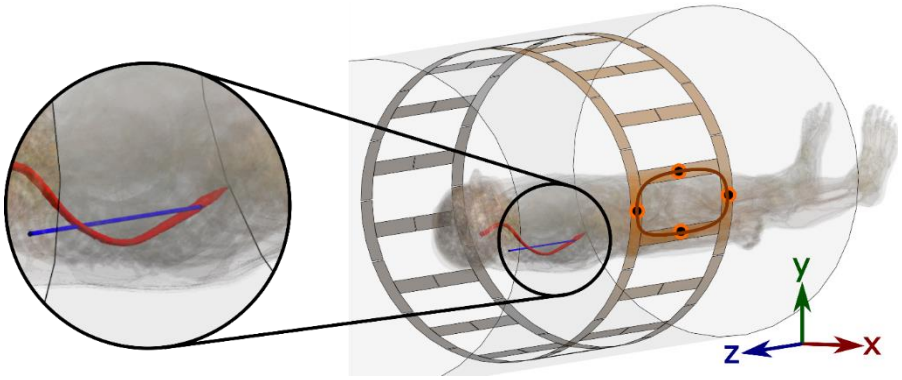


*Figure 4.3.2 Setup of 8-channel pTx coil (one channel marked by brown ring with 4 ports in orange), RF shield (grey), and human voxel model 'Duke' with a dummy stimulator implant (straight wire, blue) touching the spinal cord (red).*

*Dedicated pTx testbed*

A dedicated experimental setup (doi: 10.1002/mrm.28379) has been developed which can be used for pTx experiments at 50-300 MHz covering MRI machines from 1.5T to 7T (see Figure 4.3.3). The testbed has an 8-channel arbitrary waveform generator, eight 20 W broadband RF power amplifiers and a 4-channel receiver. For most experiments an 8-channel pTx RF coil operated at 297 MHz was used, loaded with a cylindrical PVP phantom. The receiver card (synchronised with the transmitters) was used to measure either the signals from fibreoptic field probes or RMS sensors. All pTx pulses were generated by the console, which was also controlling the positioning system COSI Measure (doi: 10.1038/s41598-017-13824-z) using a TCP/IP communication protocol. This allowed for automated 2D/3D mapping experiments of multiple implant locations.

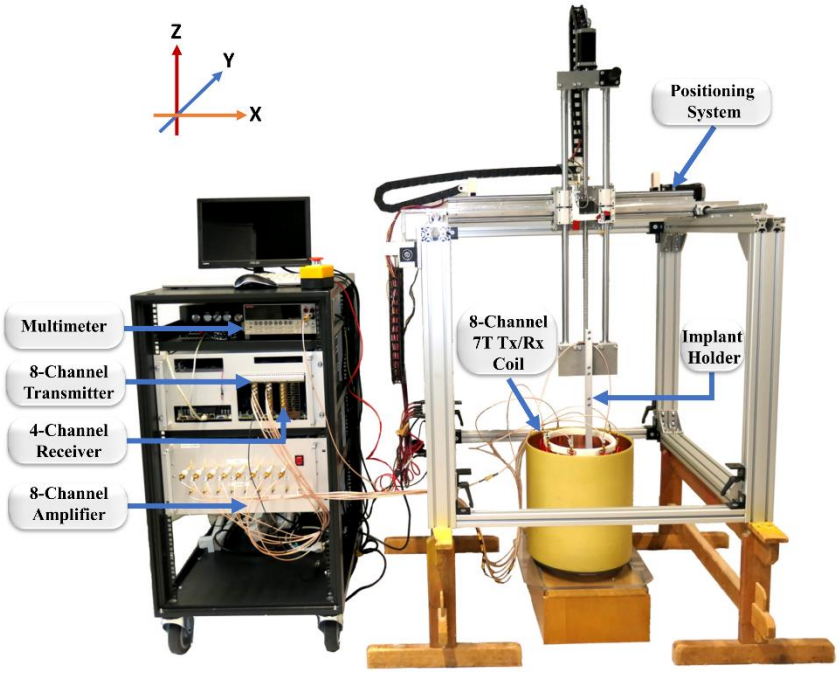


*Figure 4.3.3 Eight-channel pTx testbed configured for measurements using a 7T pTx head coil.*

*Safety concept based on smart sensor equipped implants and parallel transmission*

Within this project a new approach to implant safety in MRI was developed. The concept is based on the integration of 'native safety' (pre-calculated) and 'implant safety' requirements (determined in situ by an RMS sensor on the active implant). This is achieved by introducing normalised quantities for either contribution which then can be combined to ensure full patient safety. The feasibility of the concept was exemplarily demonstrated in silico for body imaging at 3 T using an 8-channel pTx body coil and a simplified implant resembling a neurostimulator touching the spinal cord.

In summary, the steps of the safety concept are: A) Simulations of the native case are used to derive a native safety limit. B) An implant sensor is then used to generate the sensor matrix Qs which, in conjunction with a pre-calculated sensor calibration, provides an implant safety limit. C) Combining both limits optimised safe excitations can be achieved.

In conclusion, an RF-safety concept for implant carriers was established, separating native from implant-caused hazards. Point-like RMS-sensors in conjunction with pre-calculated calibration curves allow to quantify the implant-related hazard in situ, for the given patient in the scanner. The combination of fast sensor-measurement and pre-calculated native limits can be exploited in a pTx-excitation to achieve safe conditions and best possible performance.

*Active pTx-based mitigation of implant heating in reference implants with embedded RMS sensors*

Several mock implants (see Figure 4.3.4) with embedded RMS sensors at the implant tip were built and used to demonstrate pTx mitigation and prediction of RF-induced heating (doi: 10.1002/mrm.28968).

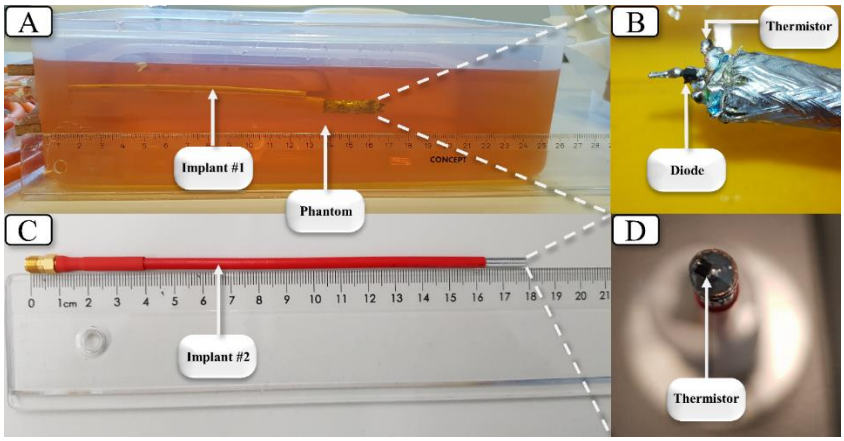


*Figure 4.3.4 Mock implants with embedded RMS sensors at the implant tip (diode and thermistor) for pTx mitigation and prediction of RF-induced heating. (A) CAT-8 cable inside a PVP filled phantom with (B) embedded diode and thermistors at its tip. (C) Photograph of a 180 mm long coaxial cable with (D) embedded thermistor at the tip.*

Since for an elongated implant like an electrode or lead, the SAR hotspot is usually found at the distal tip of the implant a safety-relevant physical quantity, e.g. E-field or temperature, can be measured at this location by a suitable sensor. The response of the implant to an pTx excitation can be described by the sensor matrix Qs which contains the full information about the implant safety. Figure 4.3.5 shows an example of the determination of the Qs matrix when using a temperature sensor.

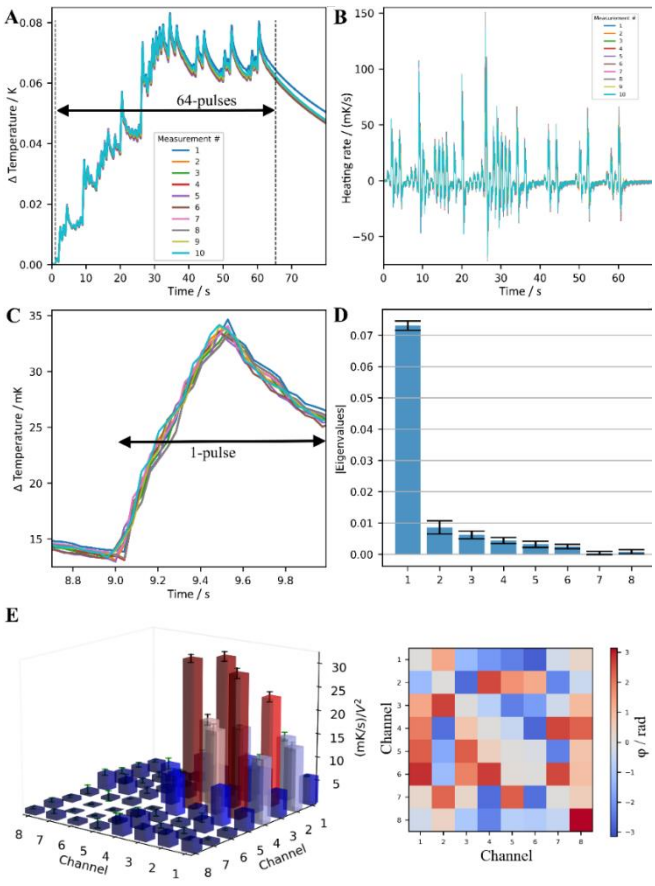


*Figure 4.3.5 Qs acquisition and repeatability based on thermistor readings in testbed experiments at 300 MHz. (A) The dashed line shows the interval of the RF pulse train. Temperature readings for 64 consecutive RF pulses of 0.5 s followed by 0.5 s of cooling after each pulse. This sequence was repeated 10 times at the same location to analyse the reproducibility of the method. (B) Heating rate dT/dt of a single Qs acquisition. (C) Single cycle thermistor readings showing the sensitivity (26 µK) and precision (100 µK) of the thermistor readings (D) Calculated eigenvalues (normalised) including standard deviation for the 10 repetitions of the Qs acquisition. (E) Amplitudes of Qs with error bars indicating the standard deviation for all repetitions and phase of Qs.*

The concept of using Qs for implant hazard mitigation is illustrated in Figure 4.3.6 where the sensor readings in an axial plane of the cylindrical phantom are shown for different excitation modes. In CP mode (circular polarisation, i.e., the standard MRI transmit mode), the sensor signal (A), i.e., $E_{rms}$ at the tip, is higher in implant locations near the phantom wall while a local minimum occurs in the central region. The measured heating rate (B) corresponds well with the measured $E_{rms}$ sensor signal. Orthogonal Projection (OP) and Null Modes (NM) are two different mitigation approaches. In the end, the OP mitigation method performs better than NM method as can be seen in Figure 4.3.6.

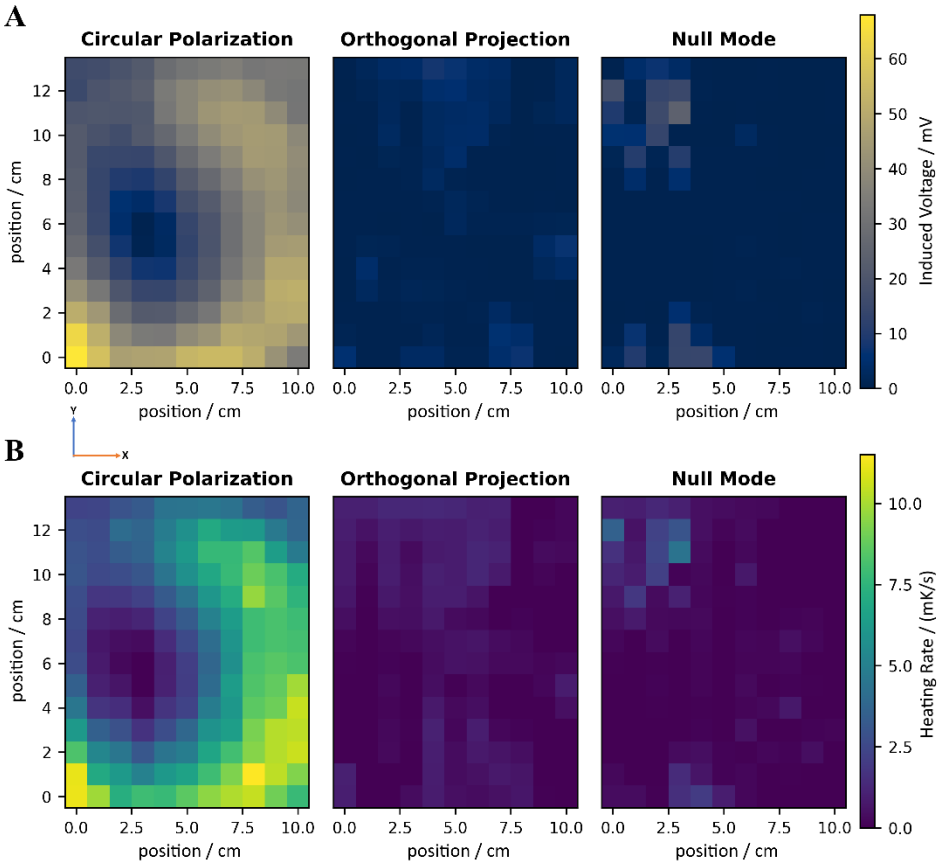


*Figure 4.3.6: Results of a Qs mapping experiment in a 110 x 140 mm2 area using the testbed at 297 MHz. The implant is immersed 120 mm into the phantom. (A) The induced voltage measurements from the modes CP, OP and NM are shown. The OP and NM are calculated and applied by using the acquired Qs. In (B) The heating rate of subsequent 2 s RF pulses using the Qs for the CP, OP and NM are shown. The induced peak voltage measured over the diode correlates linearly (R>0.94, p<0.001) with the square root of the heating rate measured with the thermistor.*

*Summary of key outputs and conclusion*

The main result presented in this report is the demonstration of the feasibility of the pTx based mitigation strategies. To this end, PTB utilised its parallel transmission medical implant safety testbed (doi: 10.1002/mrm.28379) capable of feeding an 8-channel pTx coil with calibrated individual RF voltages (amplitude/phase). Further, to assess the efficiency of sensor based pTx mitigation schemes, thermal validation measurements were performed by PTB for different exposure scenarios during sensor based pTx mitigation of implant heating. Hazard prediction, monitoring and pTx-based mitigation using RMS sensors were demonstrated both in benchtop measurements at 297 MHz and within a 3T MRI. The results presented here suggest that smart implants with embedded sensors, communicating with a scanner, may well be a promising concept towards safe scanning of patients with implants. While this work demonstrates the principal feasibility of the “smart implant” approach, it does not yet present a practical solution.

The key output of this project for the objective mitigation of implant induced hazards using real-time sensor measurements and parallel transmit radiofrequency is the following:

(i) Using simplified numerical models of wire-type implants, fully comprehensive simulations can be performed on clinically relevant body models for the pTx case. This includes established reference implants like SAIMD-U.

(ii) A simulation framework can be established that allows the risk assessment of implants in the pTx case while still being manageable in terms of resource use and can therefore be implemented by manufacturers in a similar way.

(iii) A clinically relevant safety concept based on smart sensor equipped implants can be utilised for active E-field control in the presence of metallic implants using pTx. It was shown that the proper incorporation of a single sensor signal is sufficient to cover implant safety. Without operator interaction, the procedure provides high MR imaging performance as given by mean($B_1^+$) even for strict sensor limits.

(iv) A technical implementation of this novel safety strategy for pTx-based MR systems is presented; based on RMS sensors embedded in an implant and the Qs. formalism.

(v) Using this strategy RF-induced heating could be successfully mitigated in mock implants, while maintaining $B_1^+$.

(vi) The proposed approach is real-time capable, patient and exam specific and solely based on the embedded sensor signals. No additional electromagnetic field simulations nor a priori safety testing in vitro is required.

### *4.4 Gradient heating*

*Relevance of the work carried out to meet the fourth objective*

Before MIMAS, the potential heating of an implant by the switched gradient fields of an MRI scanner was a largely unexplored field compared to RF heating. Although preliminary results convincingly demonstrated the existence of the problem, a widespread opinion assumed heating effects from gradient coil (GC) fields to be irrelevant and not to warrant any concern.

In MIMAS, the first ever systematic investigation of implant heating by switched gradients has been performed. This has been done by combining numerical simulations (with computational codes developed by consortium members) with validating experiments performed on real-life implants (e.g., hip, knee, and shoulder prostheses) tested both in a clinical MRI scanner under real-life imaging conditions and in a test-stand, specifically conceived to carry out systematic experiments in a controlled environment.

Objective 4 of the project has been tackled focusing the attention on the heating of the implants due to the energy deposition within the devices themselves, and its correlated effects, due to thermal diffusion, on the surrounding human tissues. This aspect differentiates GC-induced heating from RF heating (where energy is mainly deposited directly within the biological tissues surrounding the implants, whereas, as shown by INRIM in a recent letter to the editor of Magnetic Resonance in Medicine, the amount of RF energy deposited inside the metallic components of the prostheses results to be negligible). Towards the end of the project, the investigation has been also extended to explore possible implications for localised peripheral nerve stimulation (PNS) enhancement, responding to a stakeholder request from ISO 10974 JWG. On the contrary, potential safety issues related to device malfunctioning (EMC problems) for active implants were outside the scope of the project and therefore were not considered.

*Work undertaken by the partners*

The work on this objective started with a group of activities aimed at collecting the “ingredients” needed to identify the most relevant exposure scenarios. To achieve it, the partners collected the main characteristics of realistic gradient coils and data of typical GC sequences used in clinics, to generate a list of the potentially hazardous situations. The task included the development of a wide database containing the magnetic field distributions (three vector components of the field, for each single coil) produced by different gradient-coil designs. In particular, seven gradient designs, ranging from conventional clinical scanners to special-purpose designs, were considered. This database was prepared by INRIM, with support from PTB and IOR, and benefited from a Non-Disclosure Agreement (NDA) signed with a stakeholder (Esaote spa, manufacturer of special-purpose MRI scanners) which gave access to the design of an “open” scanner. This database was used to select the potentially most hazardous positions in the scanner for a patient carrying a knee/hip/shoulder metallic implant.

In parallel with the hardware analysis, an extensive examination of clinical sequences was performed by INRIM, IOR and PTB, to select the most relevant cases for a subsequent investigation. The choice fell on sequences which are in widespread clinical use, but also on sequences that were expected to be very ‘aggressive’, in terms of gradient heating, because of a high duty cycle of rapid gradient switching.

Finally, this group of preliminary activities was completed with the assessment of the prevalence of the main orthopaedic implants among the population submitted to MRI, using the clinical databases held at IOR and published data from European medical societies. With this input, IOR, with support from INRIM and PTB,

prepared a preliminary implant ranking list in relation to the expected power deposition. Once this list was completed, IOR provided INRIM and PTB with both physical samples and CAD models of the orthopaedic implants selected for the following analyses.

In order to test gradient-induced heating of metallic implants under fully controlled conditions, a new laboratory, including a gradient test-stand was designed and built at INRIM (Fig. 4.4.1). The metrological characterisation of this system was the subject of a specific report, collecting all the measurements done to check its performances. During MIMAS, this facility has been used to investigate, systematically, thermal effects of gradient coils on real metallic implants provided by IOR. This activity, important in itself, was also fundamental to collect the experimental data required to validate the numerical simulations, as well as to check, experimentally, the influence on power deposition of the most relevant parameters. Now, after the end of MIMAS, the new laboratory built at INRIM is available to offer to third parties a measurement service for heating of implants exposed to gradient fields. More in general, it can be also exploited to check the behaviour of magnetic field meters in a given and characterised field spatial gradient, possibly leading in the next future to the development of a new CMC. Besides the experimental campaign carried out at INRIM, PTB used a clinical MRI scanner to perform similar heating experiments, driven by gradient fields, in phantoms placed within a real MRI platform.

*Figure 4.4.1 The new gradient test lab at INRIM*

From the viewpoint of numerical simulations, during the project INRIM designed and implemented new computational tools to simulate in a realistic way the exposure to MRI gradient fields of a patient carrying orthopaedic prostheses. A first report on the possibility to make use of these tools to perform “virtual experiments”, i.e., numerical simulations with a high level of realism and reliability, to investigate the thermal effects of gradient fields without performing invasive measurements in vivo was selected for oral presentation at the workshop on Mathematical and Statistical Methods for Metrology – MSMM (Torino, 2019). Moreover, the details of the code implementation have been collected, together with some examples of application, in a paper published by INRIM and PTB in Physics in Medicine and Biology. The computational tools developed within MIMAS have been constantly updated and improved throughout the project. Now, in their final version, they allow to calculate the instantaneous power developed by the magnetic field inside the implant, following the time-behaviour of each single gradient signal (allowing the exchange of the roles of the three coils in the imaging process). Moreover, the transient thermal solver used to compute the temperature increase is able to consider possible thermoregulation effects in the blood perfusion and metabolic heat terms.

Exploiting the experimental data collected at INRIM and PTB, the electromagnetic-thermal code mentioned above has been validated, for the first time, against experimental data produced within the consortium, obtaining an excellent agreement. A report describing this validation has been the subject of an oral presentation given during the International Society for Magnetic Resonance in Medicine (ISMRM) conference in 2021.

Using the validated computational code developed by INRIM, a large number of simulations has been collected, based on two different approaches, not only considering the heating risk due to gradient fields, but also comparing it to the risk associated to RF-induced heating. In the first approach, a simplified analysis (suitable for virtual laboratory testing) has been carried on, considering several models of orthopaedic implants

(knee, hip, shoulder) placed within an ASTM phantom. The heating consequent to several realistic clinical sequences has been estimated and safety levels have been identified for each case, providing useful data to help deciding about the MRI exam execution or designing customised exam protocols. In particular, this pragmatic approach has allowed to rate the risk associated with both RF- and gradient-induced heating of knee/hip/shoulder implants during a given imaging protocol. To maximise the adoption of the proposed approach, a software package to classify the risk based on dosimetric data provided by the user has been made publicly available on Zenodo by INRIM and IOR. This package represents one of the most important outcomes of the research.

In the second approach, focused on anatomical human models that underwent a “virtual surgery”, dosimetric simulations have been performed in an anatomical model with hip implant, to study in detail the heating due to the superposition of gradient and RF fields, using realistic clinical sequences. This analysis, which put in evidence that, depending on the specific imaging sequence and body position within the scanner, the heating may be mainly driven by RF or GC fields, has given the content for a further paper, published by INRIM and PTB in Magnetic Resonance in Medicine. The conclusion of this paper is that risky situations may occur when a patient carrying a hip implant undergoes an MRI exam and that, in some cases, the gradient field heating may be significant. Thus, in general, exclusion criteria only based on whole-body specific absorption rate may not be sufficient to ensure patients’ safety. The work on anatomical human models has been further extended, to investigate the stability of the numerical results with respect to the way in which the “virtual surgery” is performed on the models themselves (considering, for instance, different possibilities for the soft tissues that fill the void left after the removal of some parts of bones, needed in orthopaedic surgery to implant the prostheses). Moreover, the stability of the results has been assessed also with respect to the variability of some physical parameters (e.g., thermal properties, blood perfusion), whose value can be affected by uncertainty or change depending on many factors (e.g., age or presence of pathologies).

Experiments to measure the gradient-induced heating of the implants provided by IOR using an open-bore scanner (made available by the stakeholder Esaote spa), initially planned to be performed during the project lifetime, were discarded because of the results of a dedicated computational analysis, which showed that the heating induced by such systems, when running clinical sequences, can be considered negligible.

Based on the experience gained on gradient-induced heating, INRIM designed a standardised and versatile procedure to test gradient-induced heating of implants (including implants with complex shape, like orthopaedic prostheses, where the geometrical anisotropy plays a crucial role) avoiding over-conservative assumptions. When combined with some a priori information, the outcomes of this procedure allow predicting the heating of a given implant placed in a given position within a specific MRI scanner and exposed to a specific imaging sequence. More specifically, the main attempt of the proposed approach is to decouple the testing phase of the device and the translation of the result in the clinical practice, with the aim of extending the applicability of the device characterisation to a variety of clinical operating conditions (adopted hardware, clinical sequences, etc.). Following this approach, the results of a laboratory testing (performed on the implant under test following a simplified protocol) can be translated into practical guides for radiologists, thanks to the technical information available from the scanner producer. The proposed procedure includes the definition of an “index of stress”, which quantifies the risk of heating for a given implant, placed in a specific position within a certain scanner, and exposed to a given sequence of gradient fields. This approach indicates the most appropriate laboratory test to certify MR compatibility and can be employed to check the effectiveness of possible mitigation strategies adopted to limit the power deposition and temperature increase due to GC fields. The procedure, that can be considered as the most important results of the research conducted within MIMAS on GC fields, has been disseminated towards the FDA and members of the committees that maintain standards ISO/TS 10974, ASTM F2182 and IEC 60601-2-33.

As an ancillary result, in the last part of the project INRIM has investigated the effect of gradient fields on implants in terms of possible enhancement of the electric field induced in the surrounding biological tissues, which may provoke unintentional peripheral nerve stimulation (PNS) in the patients’ body. Following an approach similar to that already adopted for the heating problem, the exposure to GC fields of a realistic human model has been simulated, with and without knee/hip/shoulder implants in the body, for different types of coils and different positions within the scanner. The analysis has shown that, depending on the specific situation, the level of the induced electric field can change significantly (increasing or decreasing), suggesting the importance to take the presence of the prostheses into account when investigating the thresholds for the onset of PNS in MRI.

*Summary of key outputs and conclusion*

Summing up, objective 4 has been fully achieved. Now, validated computational tools exist to investigate, in a realistic way, gradient-induced heating of implants in MRI, along with specific approaches to evaluate the risk for the patients and testing procedures to allow implant manufacturers to check the compatibility of their devices with MRI gradient fields.

Besides the papers published on scientific journals and a number of presentations given at conferences, the work carried out to investigate gradient-induced effects has been disseminated through many activities, including course for PhD students, seminars, and an interview, in Italian, whose recording is available on YouTube (https://youtu.be/oDN-KjbL5E4).

### *4.5 Small implants*

*Relevance of the work carried out to meet the fifth objective*

The objective of developing and applying a suitable statistical method to demonstrate MRI compliance for small orthopaedic implants without extensive testing or numerical modelling involved analysis of multiple aspects of MRI heating that could potentially affect compliance. In such a safety-critical application, it is necessary to identify the influence factors, quantify their likely ranges and/or values and associated uncertainties, evaluate the effects of each factor on the temperature rise within the implant, and assess whether the combined evidence gives sufficient confidence to make the proposed method suitable for use in this context.

*Work undertaken by the partners*

NPL, INRIM, IOR, ZMT and PTB jointly identified the influence factors associated with the heating of small implants. Two sets of factors were identified, one set for RF induced heating and one for gradient induced heating. In each case, the sets included geometric quantities, electromagnetic and thermal properties of the implant, electromagnetic and thermal properties of the surrounding tissue, and parameters associated with the electromagnetic fields generated by the scanner.

Each of the influence factors can be regarded as controllable, or uncontrollable. For instance, the detailed geometry of an implant is controlled by the manufacturer and potentially by the surgeon who fits the implant if deformation of the implant occurs during fitting, whereas the properties of the tissue immediately surrounding the implant are determined by the anatomy of the patient and hence cannot be controlled. Because the uncontrollable parameters are effectively random variables, the work undertaken on quantifying their effects has used a more statistical approach, whereas the work on the controllable parameters has used a more deterministic approach, as will be described in further detail below.

Computer simulations of parameterised simple implants undergoing MRI heating were developed by NPL (for RF heating) and INRIM (for gradient-induced heating). In each case, finite element models of the implants undergoing the procedure defined in ASTM F2182 were used to examine how geometric parameters and scan parameters affected implant heating. This procedure exposes the implant to an electromagnetic field for 900 s and then allows it to cool. The maximum temperature rise occurs at 900 s and this value has generally been used to compare the results of different models.

The simple implants were chosen by NPL, INRIM and ZMT to be representative of screws and plates, based on examples shown in medical catalogues. The screws were parameterised via their length, diameter, and tip sharpness. The plates were approximated as cuboids and were parameterised by their length, width, and thickness. Additional detailed models of screws undergoing RF heating were created to examine the effects of thread and head geometry details. These models showed that the thread and head details had little effect on heating and so a simplified form of screw was used in subsequent work.

The RF heating models showed that the screw length had more effect on heating than the diameter or the tip sharpness, and that the plate length had more effect on heating than the width or thickness. In both cases, the implants showed localised temperature rises at the ends of the device and a lower temperature rise at the midpoint. This effect occurs because any long thin object in an electric field will behave like a dipole antenna, with the power deposited by the antenna in the surrounding material at a maximum at the resonant length. The resonant length of the antenna is largely determined by the electromagnetic properties of the surrounding medium, although for truly three-dimensional objects the width and thickness of the object will also affect the length at which resonance occurs. For a surrounding material of magnetic permeability μ, electric permittivity

ϵ, electrical conductivity, and a field of frequency ω, the maximum power will be deposited in the material when the object has length

$$L = \frac{\pi\sqrt{2}}{\omega\sqrt{\mu\epsilon}}\left[1+\sqrt{1+\frac{\sigma^2}{\omega^2\epsilon^2}}\right]^{-1/2}, \quad (1)$$

which is half of the resonant wavelength, and integer multiples of this value. The value of this length was calculated for the properties of ASTM gel and for frequencies of 64 MHz (equivalent to a 1.5 T field) and 128 MHz (equivalent to a 3.0 T field), and were found to be consistent with the lengths of the implants that were most heated within the models. Since length was the variable of most importance, subsequent simulations were carried out using cylinders as the base geometry.

The RF heating models also looked at effects of the implant's orientation in the field, as shown in Figure 4.5.1, and the effects of placing the implant in materials with different electromagnetic properties. The variation of electromagnetic properties again showed results that were consistent with the antenna effect described above.

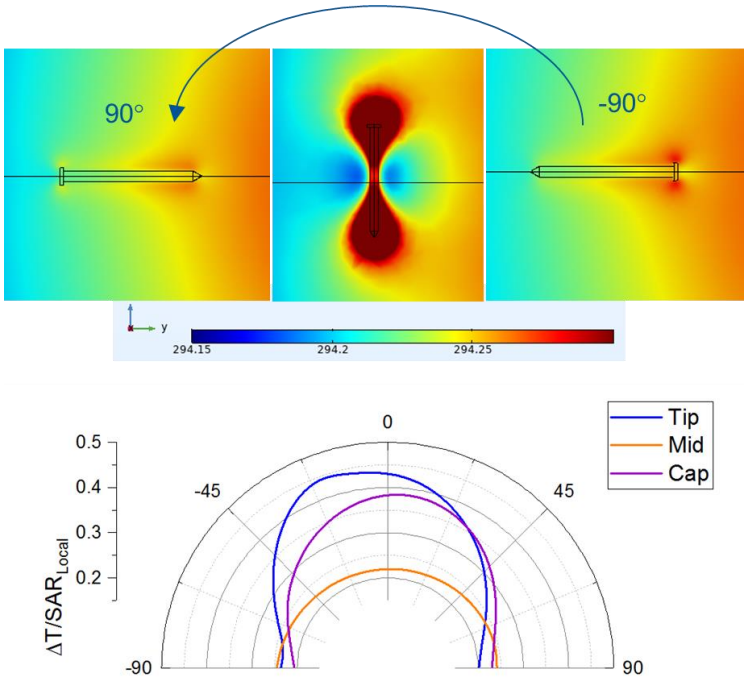


*Figure 4.5.1: Temperature distributions around screws at different orientations to the main field vector.*

NPL validated their modelling approach by carrying out a series of measurements on straight steel rods of various lengths and diameters, and carrying out simulations of these measurements. The validation process not only gave confidence in the modelling approach as agreement between measurement and model was generally very good, but also highlighted the importance of the temperature sensor position during the measurement. The antenna effect and the thermal conductivity of the gel lead to localised heating around the ends of the rods, so the sensor location is a significant source of uncertainty associated with the temperature measurement. The sensor location is also difficult to control when preparing the experiment due to the opacity of the gel. A paper reporting these results has been submitted to Magnetic Resonance in Medicine.

INRIM carried out simulations of gradient-induced heating using the same implant geometries as NPL so that results could be compared directly. This comparison has been reported in a paper published in Physics in Medicine and Biology. INRIM also carried out simulations using spheroids to explore how three-dimensional geometry affected heating, because gradient-induced heating is generated by eddy currents rather than by an antenna effect. It was found that the gradient induced heating is strongly affected by the gradient of the field at the implant position, the power index of the scan sequence, defined as

$$I_s = \sqrt{\frac{1}{T}\int_0^T \left(\frac{dG}{dt}\right)^2 dt},$$

where G is the gradient of the field and T is the total scan time, the orientation of the implant to the field, and the implant volume. Figure 4.5.2 shows a plot of implant volume against $k_p$, the deposited power normalised for scan sequence, field strength, and orientation effects, illustrating a strong correlation between the two.

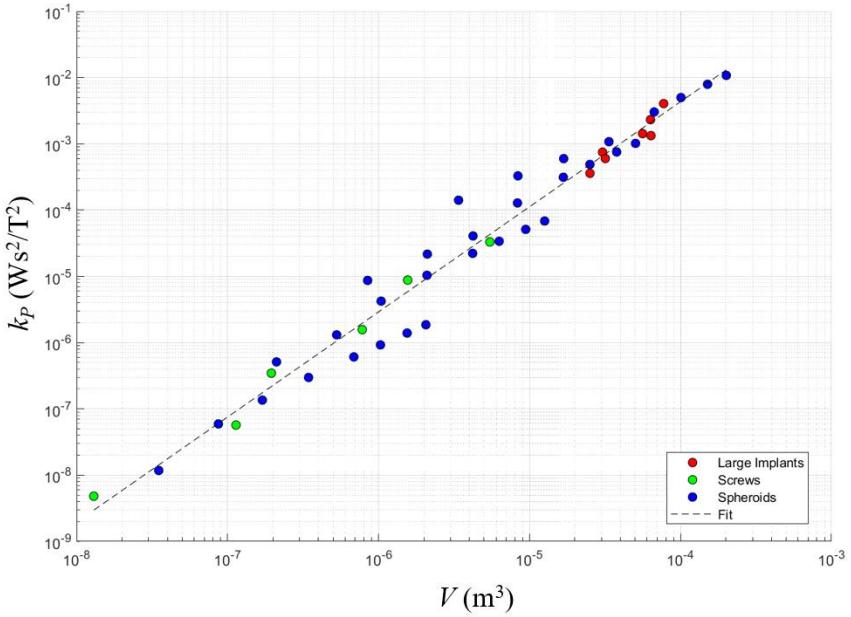


*Figure 4.5.2: Deposited power normalised for scan sequence, field strength, and orientation effects plotted against implant volume for gradient-induced heating models.*

Attempts were made to fit parametric models to the RF model results and to the gradient-induced heating model results. The fitting considered the geometric parameters for the simple implant shapes, and attempted to fit multivariate polynomials to the maximum temperature rise values calculated by the models. The attempts were only partially successful. The best fitting results for the RF models of cylindrical implants are shown in Figure 4.5.3, for a field of 1.5 T on the left and 3 T on the right. Each line represents a slice through a polynomial function of length and diameter, as described in the caption, and the symbols show the RF model results used in the fitting. The results for the RF cuboids were fitted fairly well (results not shown), but the polynomials under-predicted the temperature rise for longer implants at 1.5 T and 3 T. The gradient-induced heating model results were not well fitted by polynomials, and no suitable alternative parametric models could be identified.

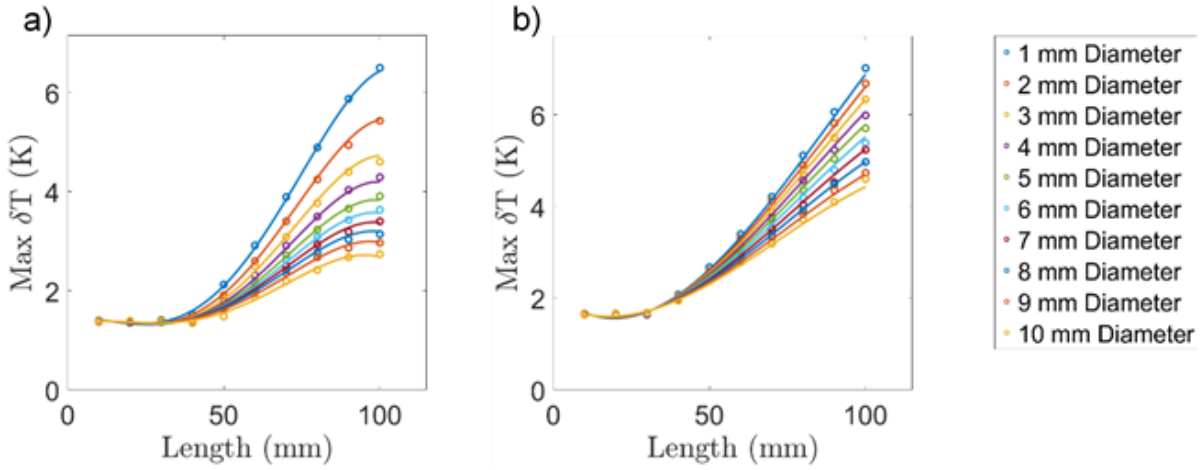


*Figure 4.5.3: Parametric models for cylinder heating after 900 seconds. Each figure shows the projection of a 2D fit onto a single plane. a) Temperature rise for a field of 1.5 T. The model has a degree of 1 for diameter and 3 for length. b) Temperature rise for a field of 3.0 T. The model has a degree of 3 for diameter and 4 for length.*

The uncontrollable parameters were treated statistically by considering variability. The variability of the tissue properties surrounding implants was considered for RF heating by ZMT and NPL. ZMT extracted maximum 10 g-averaged electrical field (E10g) from models of two of their realistic human models (Glenn and Yoon-sun) undergoing scans using ten different birdcage coils. The results were extracted at from six regions of interest (hip, knee, and shoulder on each side) for 17 positions of the human model within the scanner. Results suggested that the coil configuration only had a small effect on the value of E10g, and that there were significant differences between the values of E10g for Glenn and those for Yoon-sun, due to the differences in anatomy.

ZMT extracted the material properties within each region of interest, and NPL analysed this data to identify the differences between the two models. In general, it was observed that Yoon-sun had much higher levels of fat in all six regions of interest, and Glenn had higher levels of muscle. The averaged electrical conductivity was then used by NPL to estimate the SAR during some typical scan sequences to assess the effects of scan sequence. These effects were very significant, with the highest vales of SAR being associated with sequences with high numbers of pulses repetitions with high flip angles. Publicly available data was used by NPL to estimate the likelihood of a person with a hip or knee implant undergoing an MRI scan to clarify how frequently patients would be exposed to this level of SAR.

The uncontrollable effect of perfusion was investigated by NPL and INRIM. NPL used an idealised thermal model of a plate sitting on a bone surrounded by tissue. The thermal properties of the bone and the tissue were calculated from averages of the data extracted from their detailed human models by ZMT. The heating of the plate was simulated as two cases: in the first case, the power was deposited uniformly within the plate, and in the second the same total power was deposited in the ends of the plate. The first case is likely to resemble gradient-induced heating and the second is likely to resemble RF-induced heating. The perfusion was simulated as either constant or temperature-dependent, with values for the perfusion constant being derived from values extracted from the ZMT model and the temperature dependence being based on literature values. Two additional cases with no perfusion were simulated for reference. Figure 4.5.4 shows typical temperature rises for all six models. The values of these temperature rises were used to estimate correction factors: in all cases, the models with perfusion reduced the maximum temperature rise to between 0.85 and 0.95 times the value with no perfusion present. INRIM performed simulations using realistic implants in ZMT's human models, and found that removing perfusion increased temperature rise by between 3 % and 15 %, depending on the model used.

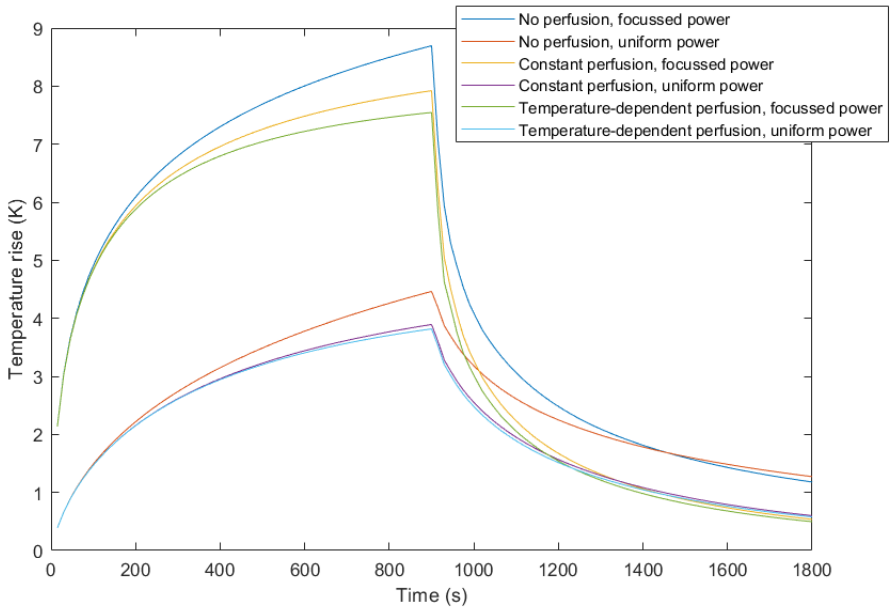


*Figure 4.5.4: Temperature rises for all six models used to study perfusion.*

*Summary of key outputs and conclusion*

All of the evidence above was combined to assess the possibility of a stochastic approach to MRI safety for small implants. It was concluded that this type of approach is not currently feasible, because:

- many of the sources of uncertainty are extremely difficult to quantify,
- parametric models that can predict implant heating accurately have not been developed even for simple cases,
- the models that can predict implant heating accurately are “black box” and computationally expensive so are not suitable for uncertainty evaluation.

# 5 Impact

MIMAS results have led to several journal papers, most notably an invited review paper and a book chapter on implant safety co-authored by multiple consortium members. Project findings were disseminated in 51 conference contributions, about one third of which were invited oral presentations. Lectures on gradient-induced heating of implants were given for PhD students in Engineering and for students of a Health Physics course.

In September 2021, an international stakeholder workshop was organised with 200 registrants from five continents and a strong (42 %) participation by industry. At this workshop, convenors and spokespersons for the most important MR safety standards ISO/TS 10974, IEC 60601-2-33, and ASTM F2182, as well as industry representatives from major manufacturers or academic researchers, gave presentations. A broad stakeholder community learned about project results and discussed the consecutive needs for the ongoing current standardization work.

*Impact on industrial and other user communities*

In December 2019, ZMT’s in-vivo RF-exposure libraries *MRIxVIP 1.5* and *MRIxVIP 3.0T* and the standardised evaluation tool *IMAnalytics* were qualified, as the first computational tool ever, by the U.S. Food and Drug Administration (FDA) as a Medical Device Development Tool (MDDT). This is a major success, since the MDDT label certified that evaluations of the health risk posed by medical implants to patients undergoing MRI were traceable, easy-to-conduct, and standardised at the most comprehensive level. The combination of *IMAnalytics* and *MRIxViP* data libraries enables the medical device industry to accelerate their approval processes with standardised risk evaluations of approved, high quality.

At the end of 2019, IMAnalytics v3.0 was released. In addition to Tier 3 (mostly for active implants), this new update now also supports Tier 2 evaluations (mostly for passive implants) with a workflow for extracting field data from the MRIxViP libraries in customised regions of interest, with derivation of all statistics necessary for Tier 2 of ISO/TS 10974. The development of this functionality enabled the quantification of worst-case *E*-fields in the human body in implant regions, which played a key part in MIMAS deliverables. IMAnalytics v3.0 and MRIxViP v2.1 have been qualified by the FDA in May 2021.

The new laboratory devoted to gradient-induced heating is now available to offer to third parties a measurement service for heating of implants exposed to gradient fields. More in general, the same facilities can be exploited to check the behaviour of magnetic field meters in a given and characterised field spatial gradient, possibly leading to the development of a new CMC in the near future.

*Impact on the metrology and scientific communities*

The successful cooperation within the MIMAS project and the deeper insight into mutual research interests and capacities led consortium members to join forces in a different research field, too. MIMAS partners were the key drivers in conceiving and procuring a new joint research project on quantitative imaging which will be coordinated by a MIMAS consortium member.

The scientific community learned about the newly developed methodologies through journal publications and conference presentations. For the first time ever, numerical models of tissue and implant heating in MRI, which were already in widespread use in the research community, are supported by a metrological underpinning.

A software package that allows the user to classify the risk associated with the exposure of bulky implants to RF and gradient fields, based on dosimetric data provided by the user himself, was made freely available to the scientific and clinical community.

*Impact on relevant standards*

The Technical Specification ISO/TS 10974 on MRI safety of active medical implants is still lacking key procedures necessary for progression to a standard. The project developed specific procedures and validated tools for the safety assessment of implants and provided a metrological underpinning to ensure that ISO/TS 10974 will i) become a full standard and ii) be continuously developed and improved. This will also contribute to the future development of IEC 60601-2-33, the international standard on MRI equipment and safety, since a complementary co-development of both the MRI and the implants standard was agreed upon by a joint ISO/IEC working group.

The procedure specifically developed in the project to test, in a standardised way, the heating of bulky implants exposed to gradient-fields was circulated and, in particular, disseminated towards the FDA and members of the committees that maintain standards ISO/TS 10974, ASTM F2182 and IEC 60601-2-33.

*Longer-term economic, social, and environmental impacts*

European implant manufacturers benefit from a faster market introduction of their innovative products as metrologically approved methods to assess the MRI safety of medical implants are now available. This holds particularly for the simulation-based assessment of active implanted medical devices (AIMD) with long electrodes or leads since these are the most hazardous implants in MRI for which new *Medical Device Development Tools* were developed and approved.

In addition, an independent, novel safety concept towards a personalised safety assessment for AIMD carriers in MRI was developed within MIMAS and the proof-of-principle was given. This approach utilises the information from sensors on the implant to adjust the RF settings of a parallel-transmit capable MR scanner. No longer the MRI operators in the clinics but rather the implant and scanner manufacturers would be chiefly responsible for the safety of implant carriers, then. The concept assigns new responsibilities, and it requires technical changes to both implants and MRI scanners. Manufacturers may be reluctant to adopt it, therefore, and even after the concept was developed and its principal feasibility demonstrated within MIMAS, the route towards formal approval and practical implementation may still be a long and tedious one. Once it is adopted, however, it will change the MR scanning of implant patients forever.

# 6 List of publications


[1] *In silico evaluation of the thermal stress induced by MRI switched gradient fields in patients with metallic hip implant.* Arduino A, Bottauscio O, Brühl R, Chiampi M, Zilberti L. Phys Med Biol. 2019. https://doi.org/10.1088/1361-6560/ab5428

[2] *RF-induced heating of metallic implants simulated as PEC: Is there something missing?* Zilberti L., Zanovello U., Arduino A., Bottauscio O., Chiampi M. Magn Reson Med 2020. https://doi.org/10.1002/mrm.28512

[3] *MRI-Related Heating of Implants and Devices: A Review. Winter* L, Seifert F, Zilberti L, Murbach M, Ittermann B. J Magn Reson Imaging 2020. https://doi.org/10.1002/jmri.27194

[4] *Parallel transmission medical implant safety testbed: Real-time mitigation of RF induced tip heating using time-domain E-field sensors.* Winter L, Silemek B, Petzold J, Pfeiffer H, Hoffmann W, Seifert F, Ittermann B. Magn Reson Med 2020. https://doi.org/10.1002/mrm.28379

[5] *Heating of hip joint implants in MRI: The combined effect of RF and switched-gradient fields.* Arduino A, Zanovello U, Hand J, Zilberti L, Brühl R, Chiampi M, Bottauscio M. Magn Reson Med 2021. https://doi.org/10.1002/mrm.28666

[6] *Rapid safety assessment and mitigation of radiofrequency induced implant heating using small root mean square sensors and the sensor matrix Qs.* Silemek B, Seifert F, Petzold J, Hoffmann W, Pfeiffer H, Speck O, Rose G, Ittermann B, Winter L. Magn Reson Med 2022. https://doi.org/10.1002/mrm.28968

[7] *Gradient coil and radiofrequency induced heating of orthopaedic implants in MRI: influencing factors. Wooldridge* J, Arduino A, Zilberti L, Zanovello U, Chiampi M, Clementi V, Bottauscio O. Phys Med Biol 2021. https://doi.org/10.1088/1361-6560/ac3eab

[8] *Statistical analysis of temperature rise in passive medical implants in a magnetic resonance imaging environment.* Cox MG, Jagan K, Rajan S. NPL Report MS28, 2021. https://doi.org/10.47120/npl.MS28

[9] *Radiofrequency-induced heating of broken and abandoned implant leads during magnetic resonance examinations.* Yao A, Goren T, Samaras T, Kuster N, Kainz W. Magn Reason Med 2021. https://doi.org/10.1002/mrm.28836

[10] *Experimental and numerical optimization modelling to reduce radiofrequency-induced risks of magnetic resonance examinations on leaded implants.* Córcoles J, Yao A, Kuster N. Appl Math Modelling 2021. https://doi.org/10.1016/j.apm.2021.02.036

[11] *Induced radiofrequency fields in patients undergoing MR examinations: insights for risk assessment.* Yao A, Murbach M, Goren T, Zastrow E, Kainz W, Kuster N. Phys Med Biol 2021. https://doi.org\10.1088/1361-6560/ac212d


This list is also available here: https://www.euramet.org/repository/research-publications-repository-link/